Annual Report, SCEC Project #08004

Three-Dimensional Seismic Velocity Models of California at Multiple Scales

Clifford H. Thurber, Principal Investigator
Department of Geology and Geophysics
University of Wisconsin-Madison, Madison, WI 53706
thurber@geology.wisc.edu

Introduction

This SCEC funded research project explored the potential for developing a higher-resolution tomographic model of the Los Angeles Basin region. The starting model incorporates (spatially decimated) velocity values from the latest Harvard SCEC Community Velocity Model (CVM-H), which is imbedded within an existing Vp and Vp/Vs southern California tomographic model. This approach allows for the resolution of deeper crustal structure while retaining a high-resolution representation of the shallow structure in a unified, self-consistent model.

Data and Method

We obtained P- and S-phase data for 15,845 local events with magnitude greater than 1.5 in our study area from the Southern California Seismic Network (SCSN). We selected the events with the greatest number of P and S picks within a 1 km radius and required each master event to have at least 8 P and 2 S picks. The resulting 4,034 earthquakes are shown by gray dots in Figure 1a. In order to constrain absolute earthquake locations and shallow crustal structure, we also assembled active-source data (show by stars in Figure 1a) from the Los Angeles Regional Seismic Experiment (LARSE). The SCSN and temporary stations are shown in Figure 1b by open and filled triangles, respectively. We performed waveform cross-correlation computation for earthquake pairs using the method described in several recent southern California relocation studies (Hauksson and Shearer, 2005; Shearer et al., 2005; Lin et al., 2007). We used 8,443 P and 11,217 S differential times with correlation coefficients above 0.9 for 640 event pairs.

Our model is represented by a uniform 2 km horizontal grid in the high-resolution area of the CVM-H model and the seismically active Northridge region and 4 km elsewhere (shown in Figure 1b). The vertical nodes are positioned at 1, 3, 6, 9, 12, 15, 20, 25 and 35 km (relative to mean sea level). We apply the adaptive-mesh double-difference tomography algorithm (Zhang and Thurber, 2005) to solve for both P and S velocity models starting with the 3D CVM-H model. We used this algorithm because it allows for an irregular mesh, although we did not actually use its adaptive capability.

Results

After we obtained our final model, the root-mean-square arrival time residual drops from 0.73 s to 0.16 s, a 78% reduction. Figure 2 shows the map view slices of the P-wave velocity model for different depth slices. The three rows are for the starting CVM-H model, our model and the velocity perturbation of our model relative to the CVM-H, respectively. The white contours enclose the areas where the derivative weight sum (DWS; Thurber and Eberhart-Phillips, 1999) is greater than 100. DWS measures the sampling of each node and serves as an approximate measure of resolution (Zhang and Thurber, 2007).

Our model is generally perturbed by less than 5% from the starting CVM-H model below 6 km depth. Therefore, we focus our discussion on the uppermost crust between 1 and 6 km depth where the most significant changes happen. In Figure 3 we show the velocity cross-sections along the two LARSE lines in Figure 1. The top three figures are for LARSE 1 and the bottom three are

for LARSE 2. As in the map views, we show the starting CVM-H model (1a and 2a), our model (1b and 2b) and the velocity perturbations (1c and 2c). For the LARSE 1 line, we only present the well-resolved area from the Los Angeles Basin to the San Andreas Fault. At about 32 km, the profile cuts the Whittier fault where we see about 10% changes across, which indicates that the CVM-H may overestimate the velocities on the LA Basin side and underestimate the San Gabriel Valley side. We also see a similar perturbation across the Sierra Madre fault zone at -52 km. The profile then enters the San Gabriel Mountains, where the most significant change along this line appears with a ~40% peak perturbation centered at 2 km depth. In this area, our model shows about 6 km/s velocity at 2 km depth with a gradient to about 6.3 km/s at 6 km depth, which agrees well with the crustal structure of Fuis et al. (2001) based on seismic refraction data.

The bottom three figures show the velocity cross-sections along the LARSE 2 line. Our resolved model agrees extremely well with the results of Fuis et al. (2003) using industry reflection and borehole data and LARSE 2 reflection data (refer to Fig. 3B in Fuis et al. (2003) for comparison). The common features include low and high velocity anomalies beneath the Santa Monica Mountains.

Conclusions

In this study, we take advantage of the recent adaptive-mesh double-difference tomography algorithm to solve for new high-resolution P- and S-wave velocity models for the LA Basin area using both absolute and differential arrival times from the SCSN. Our model agrees with the results from the seismic refraction and reflection data extremely well and should be valuable for improving the SCEC CVM-H model and for earthquake relocation studies in this area.

SCEC Funded Publications

Lin, G., P. M. Shearer, E. Hauksson and C. H. Thurber, A three-dimensional crustal seismic velocity model for southern California from a composite event method, *J. Geophys. Res.*, **112**, doi: 10.1029/2007JB004977, 2007.

References

Fuis, G. S., T. Ryberg, N. J. Godfrey, D. A. Okaya, and J. M. Murphy, Crustal structure and tectonics from the Los Angeles basin to the Mojave Desert, southern California, Geology, 29, 15–18, 2001.

Fuis, G. S., et al., Fault systems of the 1971 San Fernando and 1994 Northridge earthquakes, southern California: Relocated aftershocks and seismic images from LARSE II, Geology, 31, 171–174, 2003.

Hauksson, E., and P. Shearer, Southern California hypocenter relocation with waveform crosscorrelation, Part 1: results using the double-difference method, Bull. Seismol. Soc. Am., 95, 896–903, 2005.

Lin, G., P. M. Shearer, and E. Hauksson, Applying a three-dimensional velocity model, waveform cross correlation, and cluster analysis to locate southern California seismicity from 1981 to 2005, J. Geophys. Res., 112, doi:10.1029/2007JB004,986, 2007.

Shearer, P. M., E. Hauksson, and G. Lin, Southern California hypocenter relocation with waveform cross-correlation, Part 2: results using source-specific station terms and cluster analysis, Bull. Seismol. Soc. Am., 95, 904–915, 2005.

Thurber, C., and D. Eberhart-Phillips, Local earthquake tomography with flexible gridding, Comp. Geosci., 25, 809–818, 1999.

Zhang, H., and C. Thurber, Adaptive mesh seismic tomography based on tetrahedral and Voronoi diagrams: application to Parkfield, California, J. Geophys. Res., 110, B04303, doi:10.1029/2004JB003, 186, 2005.

Zhang, H., and C. H. Thurber, Estimating the model resolution matrix for large seismic tomography problems based on Lanczos bidiagonalization with partial reorthogonalization, Geophys. J. Int., 170, 337–345, 2007.

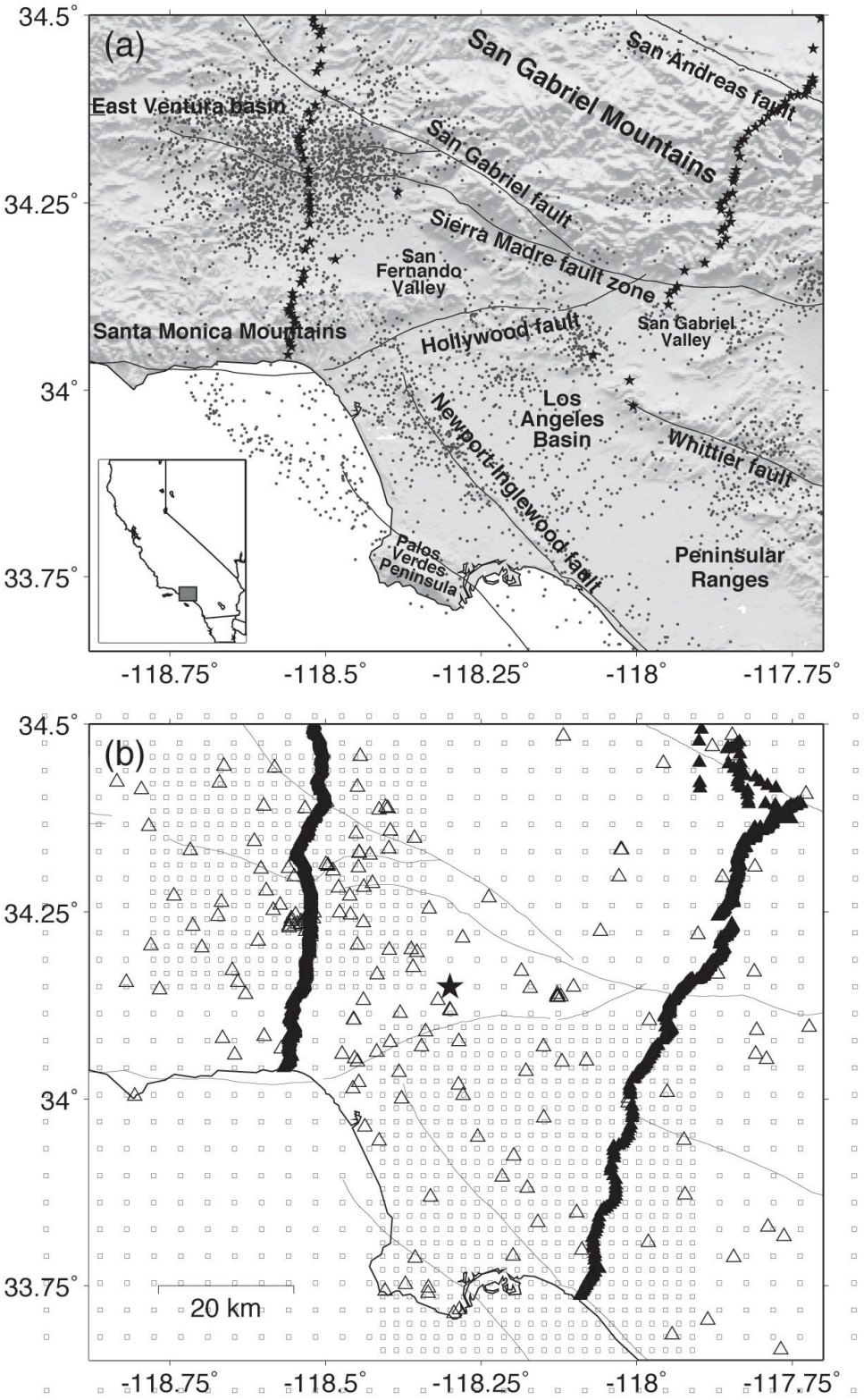

Figure 1. (a) Event distribution and some major geological features in our study area. (b) Station and inversion grid distribution. The open triangles represent the Southern California Seismic network stations and filled ones show the temporary stations in the LARSE projects.

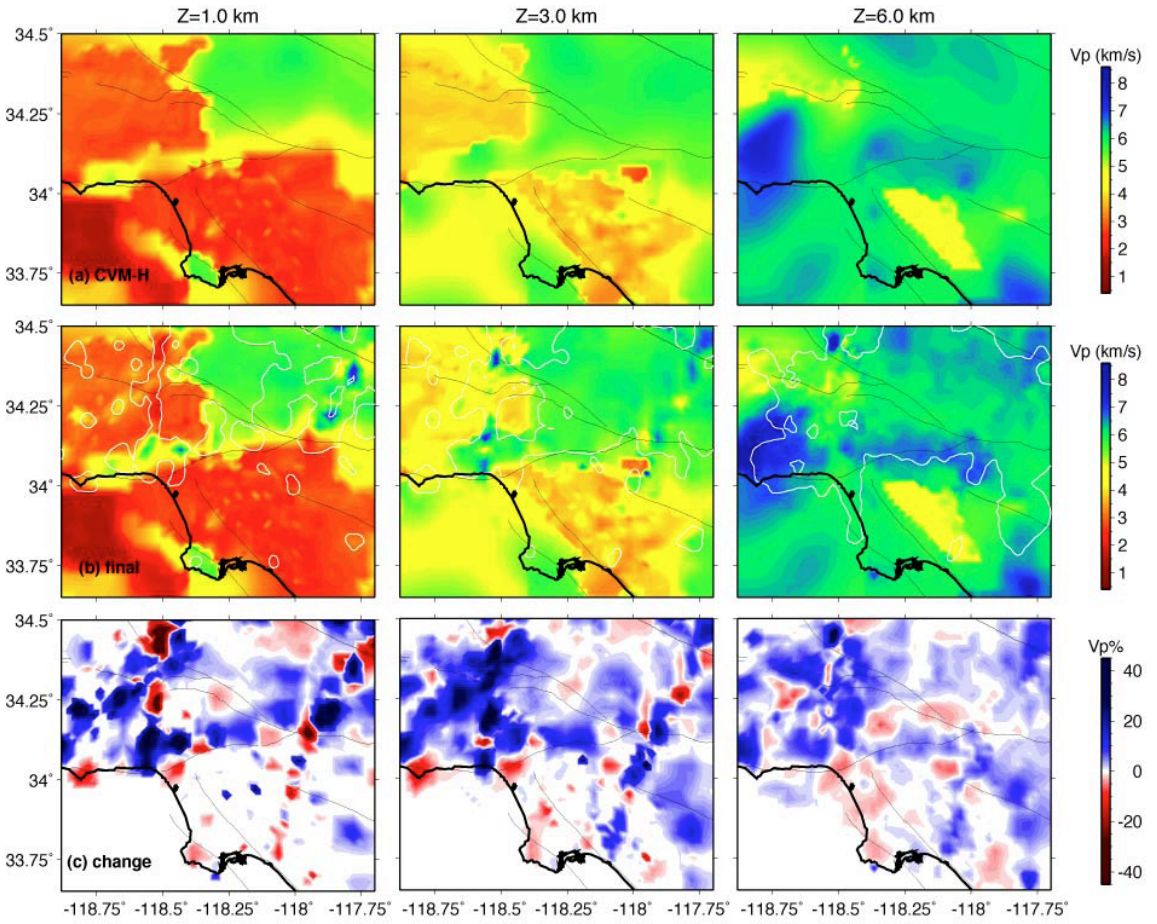

Figure 2. Map views of the P-wave velocity model for different depth slices. The three rows of panels show (top) the starting CVM-H model, (middle) our model, and (bottom) the velocity perturbation of our model relative to the CVM-H. Black lines denote coastline and lakes, gray lines rivers and surface traces of mapped faults. The white contours enclose the areas where the derivative weight sum is greater than 100.

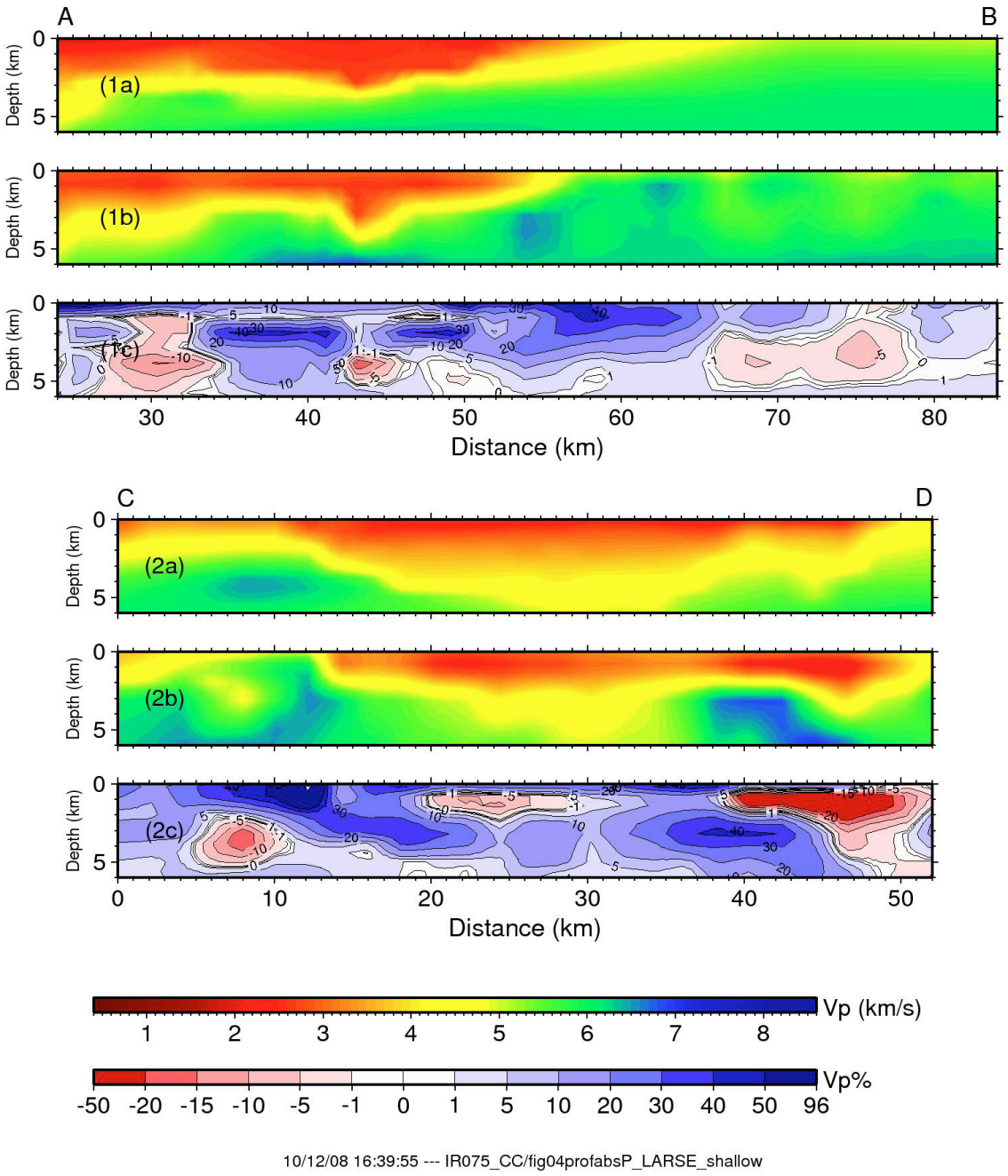

Figure 3. Cross-sections of the absolute P-wave velocity along the (top) LARSE 1 and (bottom) LARSE 2 profiles shown in Figure 1. The three rows of panels show (top) the starting CVM-H model, (middle) our model, and (bottom) the velocity perturbation of our model relative to the CVM-H.